ELSEVIER

Sensitivity of water and carbon fluxes to climate changes from 1960 to 2100 in European forest ecosystems

H. Davi [a,e,*], E. Dufrêne [a], C. Francois [a], G. Le Maire [a], D. Loustau [b], A. Bosc [b], S. Rambal [c], A. Granier [d], E. Moors [f]

[a] *Laboratoire Ecologie, Systématique et Evolution (ESE), CNRS & Université Paris Sud, Bât 362, 91405 Orsay, France*
[b] *Laboratoire d'Ecophysiologie et Nutrition, Station de Recherches Forestières, INRA Pierroton, Gazinet Cedex 33611, France*
[c] *DREAM Unit, Centre d'Ecologie Fonctionnelle et Evolutive, CNRS, 1919 route de Mende, France*
[d] *UMR INRA-UHP Ecologie et Ecophysiologie forestières, F-54280 Champenoux, France*
[e] *INRA-UR629, Recherches Forestières Méditerranéennes, Domaine Saint Paul, Site Agroparc, 84914 AVIGNON Cedex 9, France*
[f] *Alterra, P.O. Box 47, 6700 AA Wageningen, The Netherlands*

Abstract

The effects of climate changes on carbon and water fluxes are quantified using a physiologically multi-layer, process-based model containing a carbon allocation model and coupled with a soil model (CASTANEA). The model is first evaluated on four EUROFLUX sites using eddy covariance data, which provide estimates of carbon and water fluxes at the ecosystem scale. It correctly reproduces the diurnal fluxes and the seasonal pattern. Thereafter simulations were conducted on six French forest ecosystems representative of three climatic areas (oceanic, continental and Mediterranean areas) dominated by deciduous species (*Fagus sylvatica*, *Quercus robur*), coniferous species (*Pinus pinaster*, *Pinus sylvestris*) or sclerophyllous evergreen species (*Quercus ilex*). The model is driven by the results of a meteorological model (ARPEGE) following the B2 scenario of IPCC. From 1960 to 2100, the average temperature increases by 3.1 °C (30%) and the rainfall during summer decreases by 68 mm (−27%). For all the sites, between the two periods, the simulations predict on average a gross primary production (GPP) increase of 513 g(C) m^{-2} (+38%). This increase is relatively steep until 2020, followed by a slowing down of the GPP rise due to an increase of the effect of water stress. Contrary to GPP, the ecosystem respiration (R_{eco}) raises at a constant rate (350 g(C) m^{-2} i.e. 31% from 1960 to 2100). The dynamics of the net ecosystem productivity (GPP minus R_{eco}) is the consequence of the effect on both GPP and R_{eco} and differs per site. The ecosystems always remain carbon sinks; however the sink strength globally decreases for coniferous (−8%), increases for sclerophyllous evergreen (+34%) and strongly increases for deciduous forest (+67%) that largely benefits by the lengthening of the foliated period. The separately quantified effects of the main variables (temperature, length of foliated season, CO_2 fertilization, drought effect), show that the magnitude of these effects depends on the species and the climatic zone.

© 2006 Elsevier B.V. All rights reserved.

Keywords: Forest ecosystems; Carbon sink; Climate change; Canopy scale; Phenology

* Corresponding author at: INRA-UR629, Recherches Forestières Méditerranéennes, Domaine Saint Paul, Site Agroparc, 84914 AVIGNON Cedex 9, France. Tel.: +33 4 32 72 29 99; fax: +33 4 32 72 29 02.

E-mail addresses: hendrik.davi@avignon.inra.fr (H. Davi), eric.dufrene@ese.u-psud.fr (E. Dufrêne), christophe.francois@ese.u-psud.fr (C. Francois), guerric.le-maire@ese.u-psud.fr (G. Le Maire), loustau@pierroton.inra.fr (D. Loustau), alex@pierroton.inra.fr (A. Bosc), rambal@cefe.cnrs-mop.fr (S. Rambal), Agranier@nancy.inra.fr (A. Granier), Eddy.Moors@wur.nl (E. Moors).

1. Introduction

Models of the global carbon cycle that account for a dynamic terrestrial vegetation (DGVMs) predict that the global terrestrial carbon sink will increase until the middle of the 21st century (IPCC, 2001, synthesis report; White et al., 2000b; Cramer et al., 2001; Nabuurs et al., 2002). Predictions for the second half of the 21st century diverge, with some models predicting that the terrestrial carbon sink will tend to level off, while others predict a decrease (Cramer et al., 2001). Forest ecosystems play a dominant role in controlling terrestrial carbon sinks (D'Arrigo et al., 1987; Kauppi et al., 1992; Becker et al., 1994; Cannell et al., 1998; Myneni et al., 2001). In order to predict more accurately the response of the forest ecosystem carbon balance to atmospheric and climate change, we must improve our ability to understand the complex positive and negative feedbacks between climate and processes in forest ecosystems (Cramer et al., 2001).

It is now well established that rising atmospheric CO_2 concentrations and climate change influence the net ecosystem carbon balance (=net ecosystem productivity = gross primary production − autotrophic and heterotrophic respiration) in various ways. CO_2 fertilization generally enhances the leaf photosynthesis and, therefore, gross primary production (GPP). High spring temperatures induce earlier budburst for deciduous species (Badeck et al., 2004) and higher photosynthesis rate for coniferous, both allowing an increase in annual GPP. On the other hand, high temperature may increase autotrophic and heterotrophic respiration and, therefore, decrease NEP. Changes in rainfall amount and distribution (Bradley et al., 1987; IPCC, 2001, synthesis report) could increase both soil drought and evaporative demand in most regions leading to a decrease of photosynthesis (Ciais et al., 2005) and soil respiration. NEP dynamics depend on all of these processes and others, which could vary across time and space depending on climate and ecosystems properties. To quantify the changes in the terrestrial carbon sinks, an accurate description of NEP dynamics is required at the global scale. It is difficult, however, to analyse these complex interactions directly at this global scale. An essential step is to use stand scale measurements and process-based models to improve our understanding of underlying mechanisms controlling the response of forest ecosystems to atmospheric and climate change.

Numerous studies using process-based models have assessed the effects of climate changes on NEE or the net ecosystem productivity (NEP) at stand (Kirschbaum, 1999; Grant and Nalder, 2000), at regional (Häger et al., 1999; Coops and Waring, 2001; Joos et al., 2002; Minkkinen et al., 2002; Nabuurs et al., 2003) and at global scales (Sellers et al., 1997; Cramer et al., 1999; Kicklighter et al., 1999; White et al., 2000a; Cramer et al., 2001). But few studies have both evaluated the carbon process-based models at stand level against measurements and addressed the effects of climate change over the same sites as those used for validation. Because of the large number of variables and parameters included in this type of process-based models, it seems necessary to evaluate the model on the same site where the sensitivity analysis has led to confident conclusions. Moreover, all the effects are seldom separately quantified.

For our study we (1) used a process-based stand model, CASTANEA, to simulate CO_2 fluxes and carbon storage for six forest stands, (2) validated the model using eddy-flux (four sites) or stem growth data (five sites) and (3) simulated the effects of atmospheric and climatic change on the forest carbon balance at these six sites from 1960 to 2100. Our goal was to gain deeper insight into the response of forests to climate change based on a solid understanding of processes controlling current forest carbon balance. For that aim, we use CASTANEA, not as a sound predictive tool but as an analytical one, that sum up realistically all the responses of the carbon and water processes to climate change. CASTANEA simulates both the carbon and water budget at the stand scale. It couples photosynthesis, autotrophic respiration, carbon allocation, soil organic carbon and soil hydrology sub-models. It has been described in detail by Dufrêne et al. (2005) and validated for each of the component processes (photosynthesis, soil CO_2 efflux, etc.) for a beech stand (Davi et al., 2005). We adapted the phenology and allocation sub-models for sclerophyllous and coniferous evergreen forests. We used a sensitivity analysis of the model to assess the effects of climate change between 1960 and 2100 using output from the ARPEGE climate model (Déqué et al., 1998). The individual effects of CO_2, drought and temperature on NEP are separated and quantified. The sensitivity analysis was done for six stands including temperate deciduous, temperate coniferous and Mediterranean evergreen forests. In this paper, we evaluate the climate sensitivity without considering the nitrogen cycle feedbacks and nitrogen deposition changes.

Four questions are addressed in this study: Can our generic forest model accurately simulate the functioning of several forest ecosystems dominated by various tree types from deciduous broadleaved to needle-leaved evergreens? Do these ecosystems show contrasting

responses to climate change? What are the relative impacts of CO_2, temperature and drought? Does the ranking of these impacts depend on the ecosystem type?

2. Materials and methods

2.1. Model description

CASTANEA is a physiological process-based model simulating the carbon and the water balance in forest stands. The canopy is assumed to be homogeneous horizontally and is vertically subdivided into a variable number of layers (i.e. multi-layer canopy model). No between-tree variation is taken into account; i.e., one ''average'' tree is considered as representative for the whole stand. Trees are made up of five functional elements: leaves, stems, branches, coarse and fine roots. A carbohydrate storage compartment is also included, but with no physical location within the tree. The main simulated output variables are the canopy photosynthesis, maintenance and growth respiration, growth of organs, soil heterotrophic respiration, transpiration, and evapotranspiration.

Three different radiative balances are performed, in the PAR domain (400–700 nm), in NIR domain (700–2500 nm), and in the thermal infrared domain. In the PAR and NIR domains, incident irradiation is split into direct and sky diffuse radiation using equations given by Spitters (1986) and Spitters et al. (1986). The radiation extinction and diffusion are based on the SAIL model (Verhoef, 1984, 1985). In the thermal infrared the radiative balance coefficients are based on the general formalism given in François (2002) and the diffuse thermal radiation from the sky is computed from air temperature according to Idso (1981).

Half-hourly rates of gross canopy photosynthesis are calculated based on Farquhar et al. (1980) coupled with a stomatal conductance model of Ball et al. (1987). The biochemical basis of the temperature dependence of photosynthesis is based on Nolan and Smillie (1976) for electron transport rate ($V_{j\,max}$), Long (1991) for the carbon dioxide (C_i) and oxygen (O_i) concentrations at the evaporative sites, and Bernacchi et al. (2001) for all others. Leaf nitrogen effect on photosynthesis is taken into account assuming a linear relationship between the maximal carboxylation rate ($V_{c\,max}$) and leaf nitrogen content per unit area N_a, and a fixed ratio (β) between $V_{c\,max}$ and the potential rate of electron flow ($V_{j\,max}$).

Maintenance respiration depends on temperature and nitrogen content of the various organs (Ryan, 1991), while growth respiration depends on biochemical

composition of organs following the approach of Penning de Vries et al. (1974) and Penning de Vries (1975a,b). After subtraction of maintenance respiration requirements, the remaining assimilates are allocated to the growth of various plant tissues using a priority rule, which varies with the season. The heterotrophic respiration is calculated using a soil organic carbon (SOC) model (Epron et al., 2001) derived from CENTURY (Parton et al., 1987). For each run, the initial amount of carbon in the soil was determined assuming steady-state. Under this hypothesis, for each carbon pool of the soil, there is the same annual amount of carbon entering and leaving the pool. The equilibrium is calculated by a direct numerical resolution technique of the different carbon pools. The carbon pool thus estimated is dependant on the carbon inputs (leaf and woody debris, fine roots turn over), on their carbon to nitrogen ratio, on the soil temperature, on the soil humidity and on the soil type. Phenological stages (budburst, end of leaf growth, and start of leaf yellowing) and leaf growth depend on degree days.

The big-leaf Penman–Monteith equation (Monteith, 1965) is used to calculate both transpiration (Tr) and evaporation (EP). The soil water balance is calculated using a bucket model with three layers. During water stress periods, the slope of the relationship between leaf assimilation and stomatal conductance (g_1) is assumed to decrease (Sala and Tenhunen, 1996). In CASTANEA, we linearly link g_1 with the relative soil extractable water (SEW), when it falls below 0.4 (Granier et al., 1999, 2000b, see also the discussion about this threshold in Rambal et al., 2003). A complete description of the model, including equations, is given in Dufrêne et al. (2005).

The effect of CO_2 concentration is directly taken into account by the photosynthesis model. The model reproduces both, the observed enhancement of photosynthesis (Curtis, 1996) and the reduction of stomatal conductance (Beerling, 1999; Beerling and Kelly, 1997; Curtis, 1996) both due to CO_2 increase. But no other direct effect of CO_2 increase is assumed.

2.2. Model adaptation

The initial version of the model has been fully parameterised and validated against data from a beech stand (Dufrêne et al., 2005; Davi et al., 2005). Some modifications of the phenology module were made in order to use it (1) with a Mediterranean evergreen sclerophyllous (*Quercus ilex*) and (2) with coniferous species (*Pinus pinaster* and *Pinus sylvestris*).

Table 1
Main site specific input parameters of CASTANEA

	Beech	Sessile oak	Holm oak	Maritime pine	Scots pine
Slope of the dependency between V_{cmax}[a] and leaf nitrogen density	20[b]	12.7[c]	18[d]	12.9[e,f]	11.4[c,e]
Intercept of the dependency between V_{cmax} and leaf nitrogen density	0	50[c]	0	5.85[e,f]	−0.64[c,e]
Ratio between V_{cmax} and V_{jmax}[g]	2.2[b]	2.2[c]	2.1[d]	1.9[f]	2.1[c]
Quantum yield	0.292[f]	0.292[f]	0.292[f]	0.19[h]	0.19[h]
Slope of the Ball relationship	11.8[i]	11.8[i]	6.2[i]	10.8[h]	10.8[h]
Temperature effect for respiration (Q_{10})	1.84[j]	1.84[j]	2.3[k]	2.13[l]	2.13[l]
Root shoot	0.2[m]	0.2[m]	1[n]	0.2[m]	0.2[m]
Clumping factor	0.79[d]	0.79[d]	0.84[d]	0.64[o]	0.58[p]
Critical state of forcing for budburst[q]	450[r]	594[r]	913[r]	1000[r]	1100[r]

[a] The maximal carboxylation rate.
[b] Liozon et al. (2000).
[c] Medlyn and Jarvis (1999).
[d] Personal data.
[e] On hemi-surface basis.
[f] Medlyn et al. (2002) and Ehleringer and Björkman (1977).
[g] Potential rate of electron flow.
[h] Ogée et al. (2003).
[i] Medlyn et al. (2001).
[j] Damesin et al. (2002).
[k] Hoff et al. (2002).
[l] Bosc et al. (2003).
[m] Korner (1994).
[n] Rambal, S., pers. com.
[o] Guyon et al. (2003).
[p] Sternberg (1996).
[q] Temperature sum over which budburst occurs.
[r] Calibrated.

We distinguish three kinds of parameters in CASTANEA, parameters that are constant across species and sites (i.e. constants), species specific parameters, and site specific parameters. The constants are listed in Dufrêne et al. (2005). The main species specific parameters used in this study are given in Table 1 and the site specific parameters are given in Table 2.

The budburst of evergreen species is simulated based on the same method used for deciduous species (Dufrêne et al., 2005) with different values for the critical state of forcing for budburst (F_{critBB} see Table 1). The leaf fall and the evolution of the different cohorts of leaves are simulated according to empirical relationships. The rate and the date of leaf fall for the different cohorts of leaves are obtained from Rapp and Lossaint (1978) and Porté (1999) respectively for *Q. ilex* and *P. pinaster*.

During the leaf growing period, there is a priority to leaf allocation, which is prescribed by the phenology sub-model. The allocation coefficients for fine roots ($AG_{fine\ roots}$) and storage compartments ($AG_{reserves}$) are taken constant with a value calibrated on each site using long time series (see Table 4). $AG_{fine\ roots}$ is calculated by minimizing the difference between growth of fine root biomass and their mortality. In the same way, $AG_{reserves}$ is calculated by minimizing the difference between carbon allocated to the reserve pool and the carbon used from the reserve pool. The allocation coefficient for coarse roots is deduced assuming a constant ratio between coarse roots and trunks. The carbon allocation to aerial wood is thus the resultant and

Table 2
Main stand specific input parameters of CASTANEA

Site	Species	LAImax[a] ($m^2\ m^{-2}$)	LMA[b] (g(DM) m^{-2})	Nm[c] (%)	SEW[d] (mm)	B[e] (t(DM) ha^{-1})	Age (year)	Height (m)
Hesse	*F. sylvatica*	7.0	102	2.5	180	70	30	15
Le Bray	*P. pinaster*	3.2	308	1.2	110	94	29	19
Puéchabon	*Q. ilex*	2.9	224	1.2	113	66	58	6
Loobos	*P. sylvestris*	2.2	226	1.2	110	73	87	15
Fontainebleau	*F. sylvatica*	4.5	90	2.3	136	272	135	33
Fontainebleau	*Q. petraea*	7.1	108	3.0	111	235	136	33
Fontainebleau	*P. sylvestris*	5.0	226	1.4	116	183	100	24

[a] Total leaf area index.
[b] Leaf mass per area of sun leaves.
[c] Nitrogen content.
[d] Soil extractable water.
[e] Aboveground wood biomass.

is not calibrated against aerial wood growth measurements: this allows us to use it to evaluate the simulations.

Canopy clumping is more important in coniferous than in broadleaved canopies (Sternberg, 1996). It is taken into account in the model by using a clumping factor (*Agreg*) in the radiative transfer model. For each layer of leaves this factor reduces the Leaf Area used in the SAIL sub-model for the calculation of intercepted radiation.

2.3. Site characteristics

We have used four sites belonging to the Carboeuroflux network (Hesse, le Bray, Puéchabon and Loobos) in order to validate the model against eddy covariance fluxes for four different species (*Fagus sylvatica*, *Pinus pinaster*, *Quercus ilex*, *Pinus sylvestris*) in four contrasting climates. In addition, we tested the model using tree growth data from three contrasted stands dominated respectively by *Q. petraea*, *F. sylvatica* and *P. sylvestris* in the Fontainebleau forest south east of Paris. Also note that the Loobos site located in the Netherlands, which was used for the validation, was not used for the long-term, future climate simulations. For each stand used in the paper, the site description is reported in Appendix A.

2.4. Model validation

2.4.1. Eddy covariance data set

The experimental sites that provided the data were equipped following the requirements of the EUROFLUX network (Valentini, 1999). The CO_2 and H_2O fluxes were measured in meteorological towers using the eddy covariance method (Leuning and Moncrieff, 1990; Montcrieff et al., 1996; Aubinet et al., 2000). All other details can be found in Granier et al. (2000a) for Hesse, Berbigier et al. (2001) for le Bray, Reichstein et al. (2002) for Puéchabon and Dolman et al. (2002) for Loobos.

Reichstein et al. (2002) found that the Ball et al. (1987) relationship, coupling the leaf stomatal conductance with the photosynthesis, is not able to reproduce the drought effect in several Mediterranean ecosystems including Puéchabon. As CASTANEA uses the same approach we have tested its capacity to assess the water stress in this kind of ecosystem. We have also compared the net ecosystem productivity (NEP) and the evapotranspiration (ETR) simulated and measured in Puéchabon during the same periods chosen by Reichstein et al. (2002): in 1998 during the drought (between

15 August and 4 September) and after soil water recovery (between 25 September and 15 October).

2.4.2. The growth data set

The growth data were used to evaluate the capacity of the model to reproduce the productivity of the studied forests. Long-term data are available for 5 stands: for *F. sylvatica* and *Q. petraea* stands in Fontainebleau, in Hesse (*F. sylvatica*), in Puéchabon (*Q. ilex*) and in Le Bray (*P. pinaster*).

In Fontainebleau and Hesse, aerial wood growth was estimated from the measurements of the ring width of thirty dominant trees per stand, bored in Fontainebleau (Barbaroux, 2002) and cut in Hesse (Bouriaud, 2003). The radial growth of *Q. ilex* has been measured each year since 1984 on 463 trees spread over the flux tower study site (Enjalbal, 1994). The volume of aerial wood growth at stand scale is then calculated annually, using allometric relationships, diameter distributions and tree heights at various age classes (Barbaroux, 2002; Bouriaud, 2003). In order to compare the model simulations with the volume growth, we converted it into dry biomass by using a species-specific wood density value (Barbaroux, 2002).

2.4.3. The model simulations and result analysis

To analyse the generality and the accuracy of the model in predicting the carbon and water balances of different forests, the simulations were compared to both eddy covariance and stem growth data measurements. In the comparison with the eddy covariance data, the daily net ecosystem productivity (NEP = −NEE), the diurnal net ecosystem productivity (sum of fluxes during a day when PAR was above 10 μmol (photon) $m^{-2}\,s^{-1}$) and the evapotranspiration (ETR) during days without rain were further studied (Table 3). When measured and simulated ETR are compared, the days with rain have been removed since ETR is prone to measurement errors during rain events (Baldocchi and Vogel, 1996; Meiresonne et al., 2003; Davi et al., 2005). The diurnal NEP is analysed separately because the quality of the measurements is better during the day than during the night due to the limited turbulence under stable atmospheric conditions that mainly occur during the nights (Baldocchi, 2003). To allow a statistical comparison between simulated and measured values at a daily time resolution, four coefficients were used: the correlation coefficient (R^2), the root mean square error (R.M.S.E.), the systematic root mean square error (R.M.S.E.s) and the mean bias (*B*). For the first three coefficients, the definition and a discussion about their meaning are given in Kramer et al. (2002). We added the

Table 3

Goodness of fit of the model predictions expressed as explained variance (R^2), systematic root mean square error (R.M.S.E.s), total root mean square error (R.M.S.E.) and mean bias in % of daily net ecosystem productivity (NEP in g(C) m^{-2} day^{-1}) and evapotranspiration during days without rain (ETR in mm day^{-1})

	NEP					ETR				
	n	R^2	R.M.S.E.	R.M.S.E.s	Bias	n	R^2	R.M.S.E.	R.M.S.E.s	Bias
Hesse	365	0.90	1.28	0.57	−6.0	151	0.91	0.62	0.43	+24.1
Bray	365	0.72	1.13	0.62	+15.0	142	0.42	0.96	0.33	+11.7
Puéchabon	294	0.48	1.21	0.88	−5.6	297	0.65	0.35	0.14	+10.6
Loobos	294	0.69	1.03	0.38	+7.2	165	0.87	0.23	0.13	−5.0

mean bias, which is simply defined as:

$$B = \frac{\sum(Y_{\text{simulated}} - Y_{\text{measured}})}{\sum Y_{\text{measured}}} \times 100, \tag{1}$$

where Y is the studied variable

The comparisons are done using CO_2 and H_2O fluxes of 2001 for le Bray and Hesse. In Puéchabon, we use CO_2 fluxes of 2001 and H_2O fluxes from 1998 to 1999 (no water fluxes are available for 2001). For Loobos, we used the data from 1997.

For comparison with the growth data, all the model state variables (wood biomass, soil carbon, and soil water content) are reinitialised each year using values given in Table 2. As such, we assume that there are no carryover effects between years and no change between years in *leaf area index* dynamics is assumed (i.e. LAImax is constant across years).

2.5. Sensitivity analysis of the climate change trends

2.5.1. Meteorological data simulations

The climate simulations are made with ARPEGE model (Gibelin and Déqué, 2003) under the B2 scenario as defined by the IPCC, which is a moderate CO_2 emission scenario. The atmospheric model ARPEGE/IFS is a spectral model, which was originally developed for weather prediction by Météo France and ECMWF, the European Centre for Medium-Range Weather Forecasts (Courtier et al., 1991), and later extended to a climate version by Déqué et al. (1994, 1998) and Déqué and Piedelievre (1995). The spatial grid is about 60 km with a 0.25-day time resolution. We have chosen the grid point closest to the stands studied except for Puéchabon, where the nearest grid point is at an inappropriate elevation. The results of the ARPEGE model were evaluated by comparison between simulated and measured meteorological data, which were available on each studied site (the periods are specified in Table 4). Comparison of the climate scenario prediction with observed data for the period 1960–2000 leads to the conclusion that on average the ARPEGE model predictions provide a good reconstruction of climate and its geographical distribution, even if it smoothes the observed variability (Loustau et al., 2005). We also quantified on our sites the bias of the carbon and water simulations due to the use of the ARPEGE simulations outputs compared to the use of direct meteorological measurements. For that aim, CASTANEA simulations were made using both measured and ARPEGE simulated meteorological data (Table 5). As each type of ecosystem is characteristic of a given climatic area, it is not possible to use the same climate for all four sites, even if that would have facilitated the interpretation of the result.

Table 4

Comparison between mean simulated and measured wood growth; R^2 represents the explained variance of the annual wood growth during the period of measurements

Site/species	Period of measurements	Average measured growth (g(C) m^{-2} year^{-1})	Average simulated growth (g(C) m^{-2} year^{-1})	R^2
Hesse/beech	1980–1999	288	423	0.41
Bray/martime pine	1987–2001	428	636	0.42
Puéchabon/holm oak	1985–1993	104	170	0.83
Fontainebleau/beech	1980–2000	242	396	0.44
Fontainebleau/sessile oak	1980–2000	173	318	0.35

Table 5
Comparison of CASTANEA long-term simulations in percentage using two inputs: measured and simulated (by ARPEGE) meteorological data

	Hesse	Bray	Puéchabon	Fontainebleau
Period of measurements	1980–2000	1987–2001	1984–1998	1980–1999
Temperature	1.3	−6.5	−9.6	3.3
Rain	24.4	−20.2	−29.4	17.2
Rain in summer[a]	12.5	−4.4	0.6	10.3
Gobal radiation	−1.1	−4.7	−7.4	−13.4
Relative humidity	16.5	12.5	5.2	7.1
GPP[b]	−4.8	−3.7	5.7	1.2
Reco[c]	−0.4	−2.3	−2.6	5.3
NEP[d]	−12.7	−6.1	27.1	−6
ETR[e]	8.6	−13.7	−7.8	11.9

Results are given in percentage of bias between ARPEGE and measured data.

[a] From 1 May to 1 September.
[b] Gross primary production.
[c] Ecosystem respiration.
[d] Net ecosystem productivity.
[e] Evapotranspiration.

2.5.2. Long-term simulations of fluxes and growth

The simulations are done from 1960 to 2100 for the six stands described above. There is no simulated evolution of the stand related to the age of the stand. The state variables (wood biomass, soil carbon) are reinitialised each year. The climate and the atmospheric CO_2 effects are investigated on a stand, assuming a fixed age. The atmospheric CO_2 concentration varies with time using the following equation:

$$\text{if}(Y \leq 2000)[CO_2] = 1.48 \times (Y) - 2591.8,$$
$$\text{if}(Y > 2000)[CO_2] = 369 \times (1.00522)^{Y-2000} \quad (2)$$

The significance of the trends is tested with the Pearson test and quantified over three periods: 1960–2019, 2020–2100 and 1960–2100. Over the same periods we calculated the trend from the linear regression equations.

2.5.3. Order of importance of the various effects (CO_2, temperature, vegetation length, water stress)

One objective is to quantify separately the effects of CO_2 fertilization, soil water stress, the length of the leafy period in deciduous species and of the other climatic variables (i.e. temperature, radiation, air vapour pressure deficit) on the carbon and water fluxes. In order

to separate these effects we used five sets of simulations. The first set is a base simulation including all the effects where (i) the CO_2 concentration varies according to Eq. (2), (ii) soil water stress acts on stomatal conductance by decreasing the slope of the Ball et al. (1987) relationship, (iii) the budburst and the leaf fall are simulated depending on the degree days model and (iv) the other climatic factors (temperature, VPD, radiation) vary based on the climate scenarios. A second set of simulations assumes a constant CO_2 concentration (set to 323 ppm, which corresponds to the mean between 1960 and 1980). A third set of simulations is done without effect of the soil water stress. In the fourth set – done only for the deciduous species – both budburst and leaf fall were forced to their mean values simulated in the base simulations between 1960 and 1980. Finally in the fifth set, the CO_2 increase, water stress and phenology changes are removed, leaving only the other climatic factors as driving variables. The determination of each effect is then deduced by the comparison between the simulations of the base version and the simulations of the sets 2, 3 and 4. The climatic effects are estimated by the observed trends on the last simulation and finally, we quantify the role of each factor in the trends observed on NEP between 1960 and 2100 as follows:

$$CO_{2\,\text{effect}} = \text{rate}_{\text{base version}(1)} - \text{rate}_{\text{version without }CO_2\text{ increase}(2)},$$

$$\text{water stress}_{\text{effect}} = \text{rate}_{\text{base version }(1)} - \text{rate}_{\text{version without water stress }(3)},$$

$$\text{phenology}_{\text{effect}} = \text{rate}_{\text{base version }(1)} - \text{rate}_{\text{version without phenology change }(4)},$$

$$\text{other climatic}_{\text{effect}} = \text{rate}_{\text{version without }CO_2,\text{water stress and phenology changes }(5)},$$

$$\text{interactions}_{\text{effect}} = \text{rate}_{\text{base version }(1)} - CO_{2\,\text{effect}} - \text{water stress}_{\text{effect}} - \text{phenology}_{\text{effect}} - \text{other climatic}_{\text{effect}} \quad (3)$$

where the rate (in $g(C)$ m^{-2} $year^{-1}$) is the slope of the linear regression of the NEP between 1960 and 2100. As there are probably interactions between the different effects (water stress and phenology or water stress and CO_2 increase), we calculated the effect of these interactions such that the sum of all effects gives the real trend as simulated in the base version.

2.5.4. How climate effects alter key processes in CASTANEA?

These various effects act on the model in different ways. Rising atmospheric CO_2 stimulates the photosynthesis and reduces the stomatal conductance as a consequence of the coupling of the photosynthesis model (Farquhar et al., 1980) and the conductance model (Ball et al., 1987). Modelled photosynthesis is also sensitive to the relative humidity and to global radiation. Rising temperature modifies photosynthesis according to Bernacchi et al. (2001) and stimulates both the autotrophic and heterotrophic respirations based on Q_{10} relationships that depend on the tree species and the type of respiration (autotrophic or heterotrophic). Temperature also alters phenology depending on degree days. Finally, in the model, the precipitation controls the level and the duration of the water stress, which acts on photosynthesis, stomatal conductance, and soil heterotrophic respiration (Dufrêne et al., 2005).

3. Results

Note that in this paper a positive NEP is associated with a terrestrial sink and corresponds to a negative NEE.

3.1. Comparison with eddy covariance measurements

Results for evergreen species (Bray, Loobos, and Puéchabon sites) are presented in Fig. 1, while comparisons concerning *F. sylvatica* in Hesse are shown in Fig. 2.

In the Bray site for *P. pinaster*, the model reproduces the seasonal pattern ($R^2 = 0.76$), with a tendency to overestimate the NEP especially during autumn after the end of a drought period. For *Q. ilex* stand at Puéchabon, the model captures 60% of the variability of diurnal fluxes between days, with a tendency to slightly underestimate NEP, except in May. In May, the model overestimates photosynthesis at low values of air relative humidity. Moreover, the model fails to reproduce large peaks following strong rain events in the autumn that lead to an increase of nocturnal

respiration. For *P. sylvestris* in the Netherlands (Loobos), the model reproduces 68% of the variability but underestimates the drought effect during a short period in July. Finally for the *F. sylvatica* stand at Hesse, the model captures well the diurnal variation in NEP ($R^2 = 0.90$). When integrated over the whole year, the NEP is either overestimated for the coniferous species in Bray (+15%) and Loobos (+7%) or underestimated for the broadleaf species in Hesse (-6%) and Puechabon (-5.6%). When integrated over the whole year, the NEP is either overestimated for the coniferous species in Bray and Loobos or underestimated for the broadleaf species in Hesse and Puechabon (Table 3).

For the evapotranspiration (ETR), the model captures well the seasonal variation but except in Loobos we overestimate the total ETR (Table 3). Concerning the capacity of the model to reproduce the water stress in Puéchabon, the model simulates correctly ETR during and after water stress, except for the very low fluxes measured during the nights in the drought period (Fig. 3b). Nevertheless, the model underestimates ETR from 25 September until 15 October and thus probably overestimates the water use efficiency (WUE) here defined as the ratio between daily GPP and daily transpiration (TR). Finally, contrary to the results of Reichstein et al. (2002), the simulated WUE decreases slightly during the water stress (average WUE of 4.99 $g(C)$ dm^{-3}) when compared with the period after the drought (average WUE of 5.74 $g(C)$ dm^{-3}).

3.2. Comparison with growth data measurements

Table 4 gives the measured and simulated mean aerial wood growth and the percentage of the between years variation explained by the model for each ecosystem. Variability of aerial wood growth across ecosystems is well reproduced by the model (Fig. 4) although the mean growth is systematically overestimated (147 $g(C)$ $year^{-1}$ in average over all ecosystems). It reproduces some of the year-to-year variability (between 35% and 83%).

3.3. Simulation of the climate evolution

Table 5 shows the evaluation of the ARPEGE model on the four studied sites in current climate. ARPEGE overestimates precipitation in the Northern sites (Hesse, Fontainebleau) and underestimates it in the Southern sites (Bray, Puéchabon). Therefore, there is a strong bias in the simulation of ETR (up to 13.7%) but little effect on the gross carbon fluxes (GPP, R_{eco}, less than 5.7%).
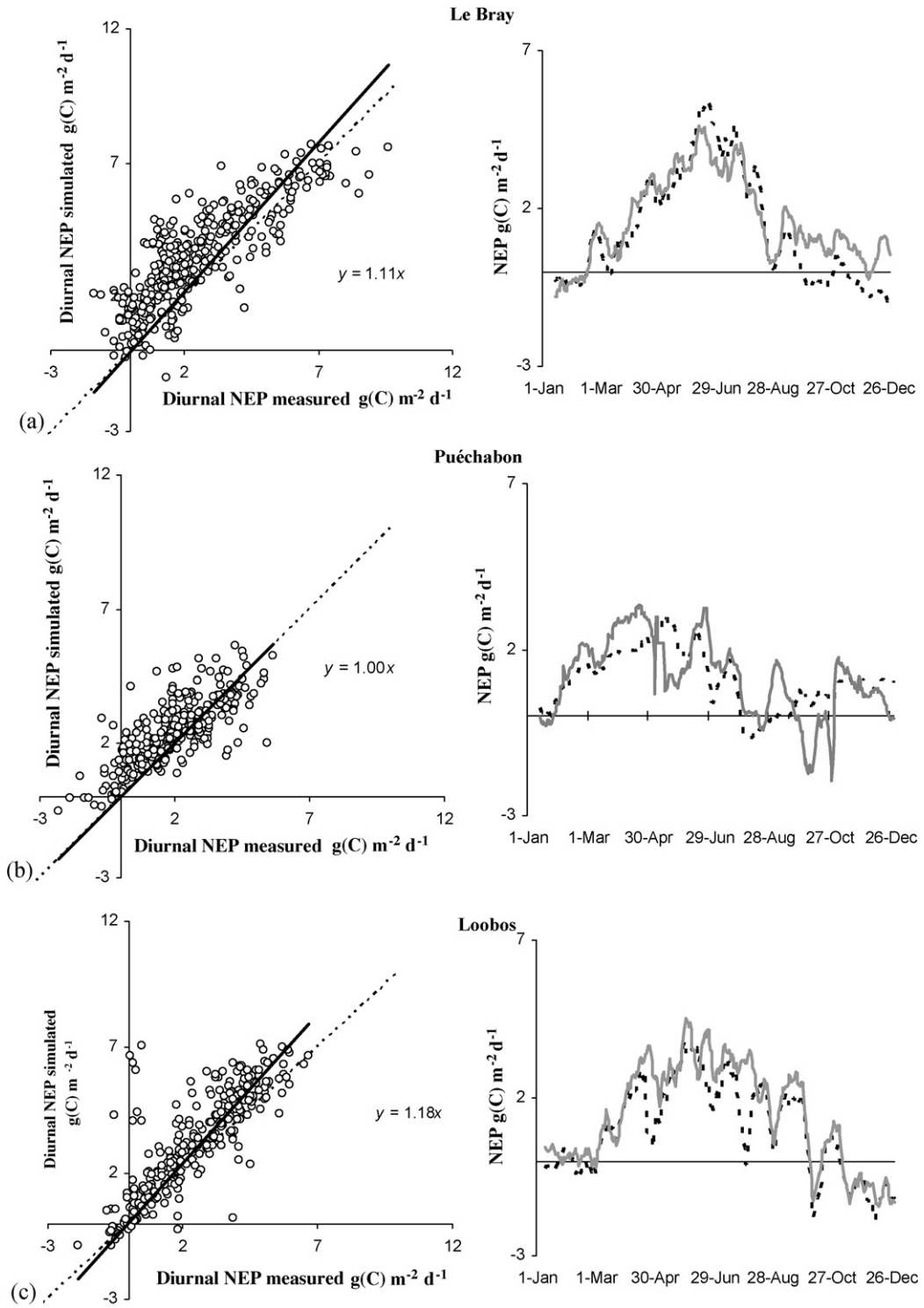
Fig. 1. Evaluation of the model predictions in evergreen species. Left: measured vs. modelled diurnal net ecosystem productivity. Right: temporal dynamics of simulated (solid line) and measured (dotted line) daily (over 24h) net ecosystem productivity (NEP, sliding average over 10 days).

Hesse 2001
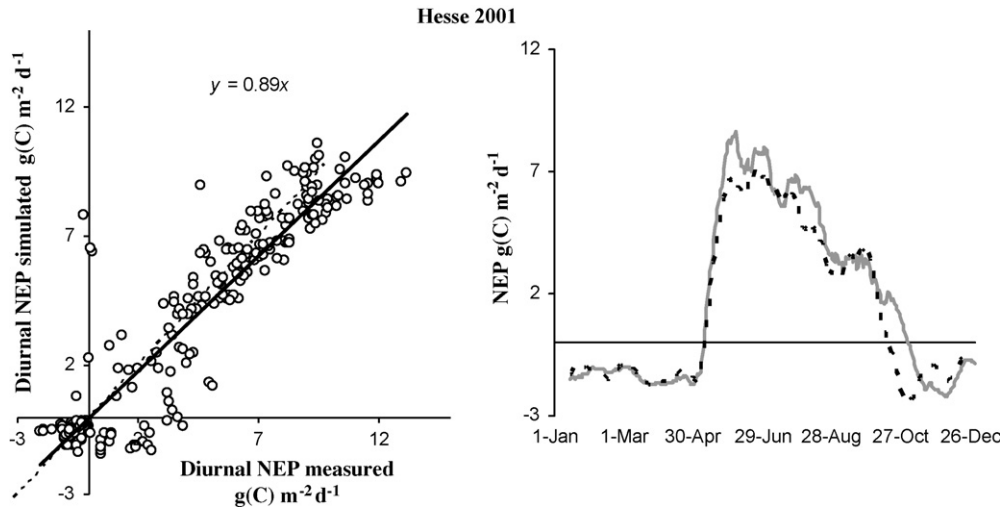
Fig. 2. Evaluation of the model predictions in a beech stand. Left: measured vs. modelled diurnal net ecosystem productivity. Right: temporal dynamics of simulated (solid line) and measured (dotted line) daily (over 24h) net ecosystem productivity (NEP, sliding average over 10 days).

However, as NEP is the difference between GPP and R_{eco}, a weak effect on one of them can have a large effect on NEP (in percentage) such as in Puéchabon or in Hesse. Some effects are largely indirect and difficult to explain: for example in Hesse even though rain, relative humidity and temperature are higher in ARPEGE simulations than measured, GPP is lower; in fact this is due to a higher ETR, which accentuates the
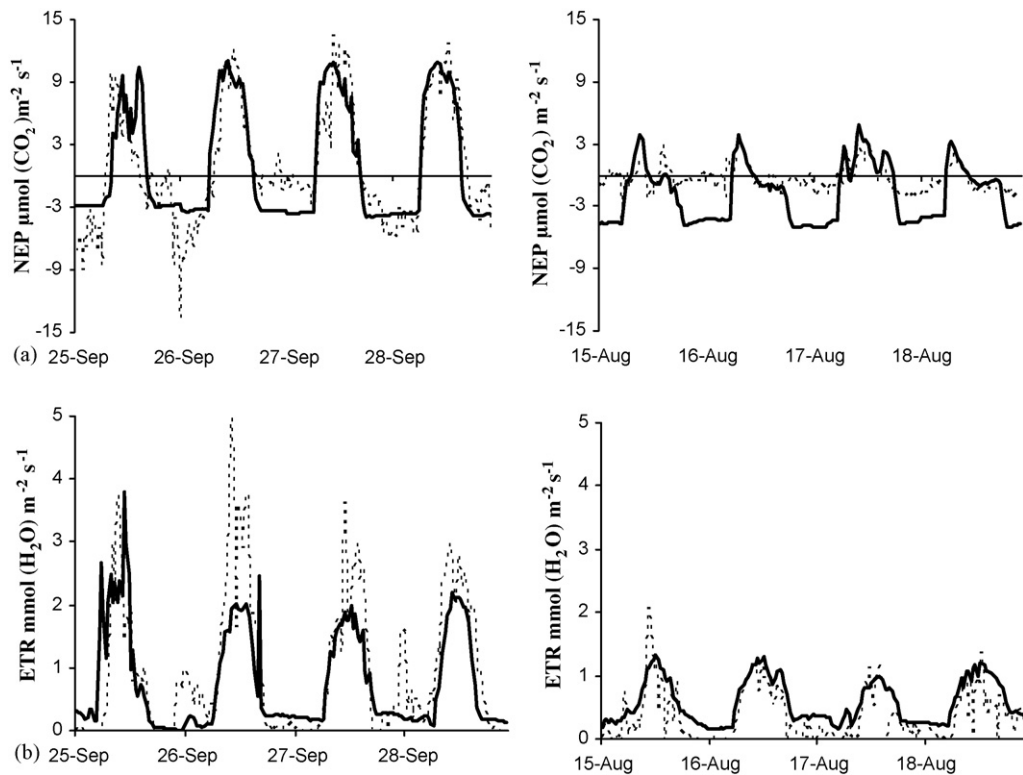
Fig. 3. Simulated (solid line) and measured (dotted line) half-hourly (a) net ecosystem productivity (NEP) and (b) evapotranspiration (ETR) 4 days during (left) and after (right) the drought period in Puéchabon.
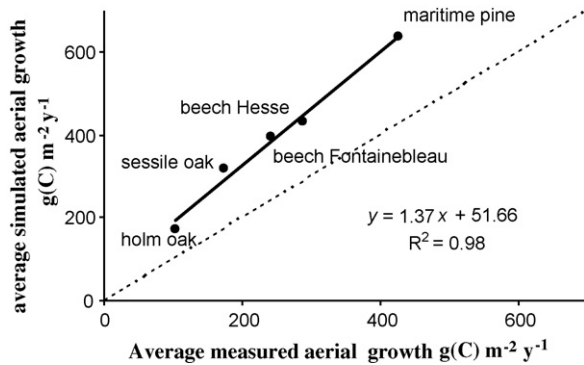
Fig. 4. Comparison of the measured and simulated average mean annual growth on five sites. The periods of measurements are given in Table 4.

water stress. The fact of over-estimating ETR with the ARPEGE meteorological simulations can cause an over-estimate of the effect of the water stress in the simulation from 1960 to 2100. These results are only indicative as such, because they compare local data to average values for a grid element. It cannot be expected to reproduce local data not only because of the known differences between climate model outputs and real weather, but also because no downscaling was used.

From 1960 to 2100 for all sites, ARPEGE simulates a significant increase of temperature ranging between 26.8% and 34.5% (from +3 to +3.3 °C) and also an increase of global radiation of about 5% (Table 6, Fig. 5). The increase of temperature mainly occurs during two distinct periods: between 2010 and 2040 and between 2060 and 2080. The summer precipitation shows no significant trend (just a slight increase) until 2020 and then strongly decreases by 33 mm (data not shown).

3.4. Sensitive analysis of carbon and water fluxes to the climate change trends

These results concern the base simulation which includes the combined CO_2, soil water stress, phenology and other climate effects. The gross primary production (GPP) quickly increases between 1960 and 2100 (Fig. 6a, Table 6), the increase is stronger in the case of the deciduous species (62% in Hesse, 41% and 54% in Fontainebleau respectively for *Q. petraea* and *F. sylvatica*) than for the evergreen species. With a GPP increase of 33%, the broadleaf evergreen species (i.e. *Q. ilex*) reaction is intermediate and between that of the deciduous and of the coniferous (19% in average) species. The model predicts that GPP will increase much less rapidly after 2020 for all stands except in Hesse and in Puéchabon.

The model also predicts a strong increase in the ecosystem respiration (R_{eco}) in all ecosystems (Fig. 6b). As for GPP, the trends are more pronounced in the case of the deciduous species for which the increase in respiration rate (average of 38%) is higher than for the evergreens (increase rate of 25%). Moreover, the time trends are very similar between species within each vegetation type (i.e. deciduous, coniferous). In contrast to GPP, the ecosystem respiration increases after 2020 at the same rate in Puéchabon or even at higher rates for the other sites than before this date (in parallel with the temperature dynamics).

As NEP is the difference between GPP and R_{eco}, a slight difference in the increase rates between GPP and R_{eco} could change the sign of the trends on NEP (Fig. 6c). The coniferous species ''benefit'' less from climate change (Table 6). Between 1960 and 2100, *P.*

Table 6
Rate (%) of meteorological trends simulated between 1960 and 2099

	Hesse, *F. sylvatica*	Bray, *P. pinaster*	Puéchabon, *Q. ilex*	Fontainebleau		
				Q. petrae	*F. sylvatica*	*P. sylvestris*
Temperature	34.5 (3 °C)	26.8 (3.3 °C)	28.3 (3.3 °C)		29.9 (3 °C)	
Rain	2	−9.3	−5.5		−3.3	
Rain during summer	−6.0 (−21 mm)	−38.9 (−100 mm)	−34.1 (−60 mm)		−28.8 (−90 mm)	
Global radiation	5.7	4.9	3.7		7.2	
Relative humidity	−2.4	−6.2	−4.4		−4.9	
GPP[a]	61.8	17.8	32.8	41.2	55.4	19.8
Reco[b]	40.7	21.1	27.0	36.1	36.7	25.8
NEP[c]	103.2	−1.8	34.0	40.9	57.3	−13.9
ETR[d]	−7.3	14.3	−1.5	−4.7	−5.3	−13.3

The significant rates are filled in grey (Pearson test).

[a] Gross primary production.
[b] Ecosystem respiration.
[c] Net ecosystem productivity.
[d] Evapotranspiration.

Fig. 5. Comparison of the average mean annual temperature (°C), global radiation (MJ), summer precipitations from 1 May to 1 September (mm) and relative humidity (%) simulated by ARPEGE models over four French sites (presented results are moving average over 10 years).

sylvestris in Fontainebleau has an overall significant decrease of NEP (−14%) and *P. pinaster* does not show significant trends. The model predicts a significant increase of NEP for the stands dominated by broad-leaved species, whose rate varies greatly: from 34% in Puéchabon, 49% in Fontainebleau (in average for *F. sylvatica* and *Q. petraea*) and up to 103% in Hesse. We have also observed the potential effects of climate changes on the aerial wood growth. It shows no significant trends for the coniferous species neither for *Q. petraea* in Fontainebleau. On the other hand, the growth is stimulated for *F. sylvatica* in Fontainebleau (+11%) in Hesse (+21%) and in *Q. ilex* coppice in Puéchabon (+12%).

In the water balance, ETR decreases of 13.7% in the coniferous stands while no significant trends are found for the broadleaves species (Fig. 7a). The ratio between transpiration and evapotranspiration decreases by 3.2% until 2020 in average for all ecosystems, only in the case

of the two coniferous stands this decline continues after 2020. As expected the water use efficiency increases strongly by about 50% (Fig. 7b). Indeed, the fertilization due to the CO_2 raise enhances GPP, without changing ETR. Moreover, as a consequence of using the Ball et al. (1987) conductance relationship without any change of its slope with the CO_2 increase, the model predicts a strong inhibition of the stomatal conductance (−39%), which above all affects ETR and to a much less extend GPP.

3.5. Order of importance of the various effects (CO₂, temperature, vegetation length, water stress) in the trends

For the deciduous species, the length of the leafy period increases by 38 days from 1960 to 2100. Early budburst contributes to 55% of this increase and the delayed leaf fall to 45%. This effect is quite linear until 2100 and it greatly contributes to the annual NEP
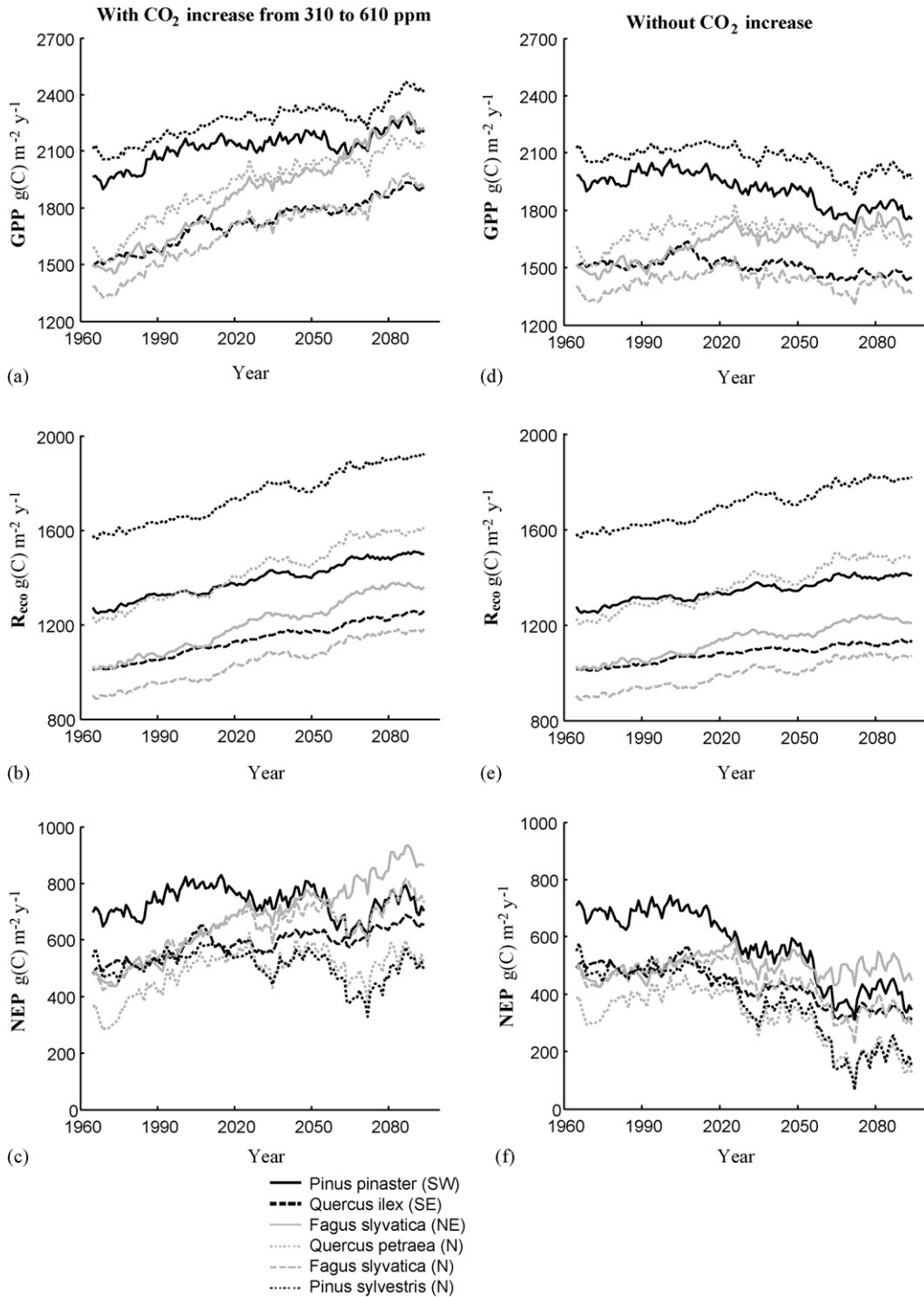
Fig. 6. (a, d) Gross primary production (GPP), (b, e) ecosystem respiration (R_{eco}) and (c, f) net ecosystem productivity (NEP) simulated from 1960 to 2100 with (left) or without (right) taking into account the atmospheric CO_2 raising (presented results are sliding average over 10 years).

increase in the case of the deciduous species (see also Fig. 8). The date of budburst contributes much stronger than the date of leaf fall, due to the high level of incoming radiation during spring for the range of

latitudes considered. In 2100 the increase of the length of the foliated period will stimulate NEP by about 150–220 g(C) m^{-2} year^{-1}. This effect is greater in Hesse than in Fontainebleau and for this last site $Q.$ $petraea$

With CO$_2$ increase from 310 to 610 ppm

Without CO$_2$ increase
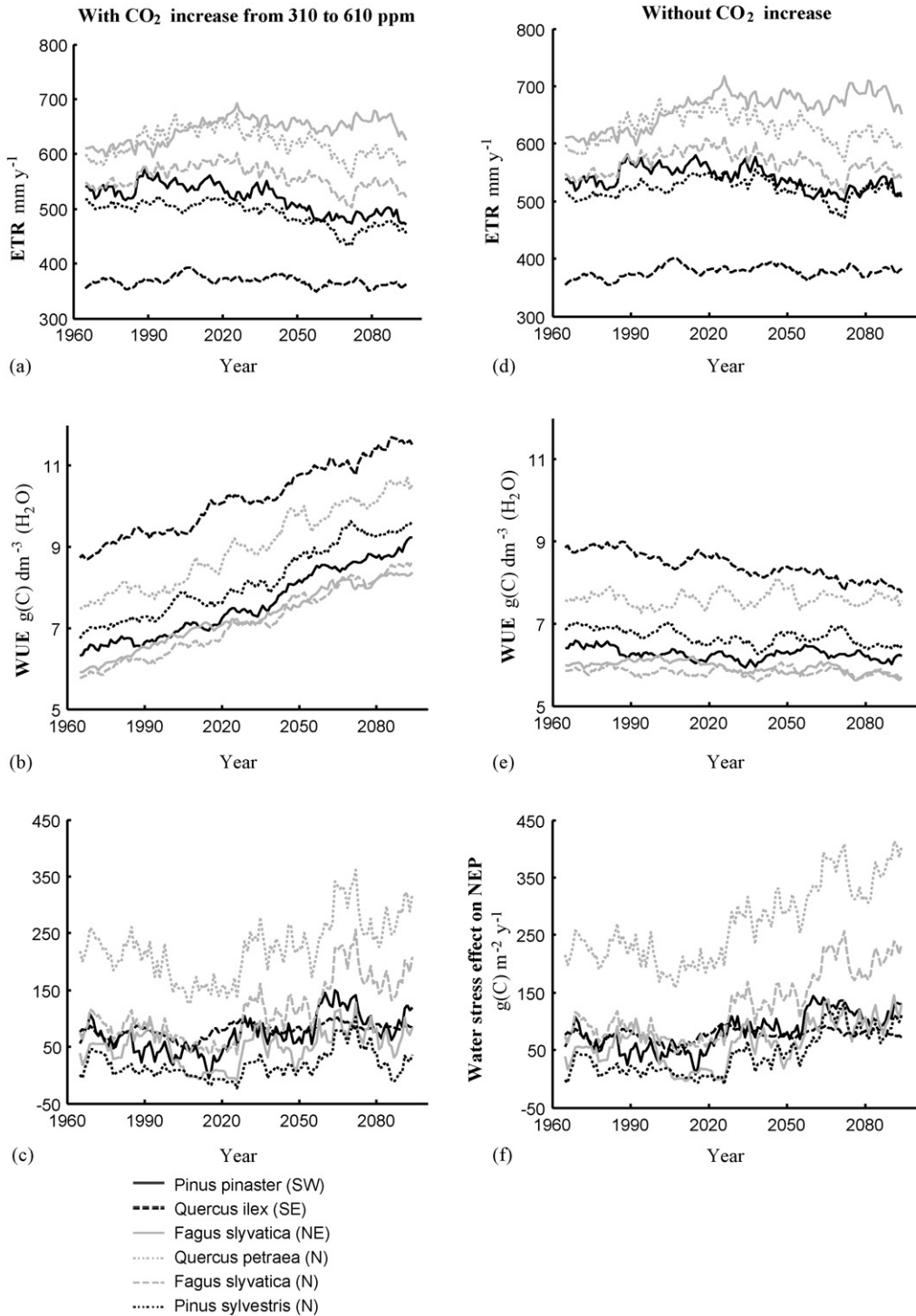
Fig. 7. (a, d) Evapotranspiration (ETR), (b, e) water use efficiency (WUE) and (c, f) the water stress effect on net ecosystem productivity simulated from 1960 to 2100 with (left) or without (right) taking into account the atmospheric CO$_2$ rising (presented results are sliding average over 10 years).
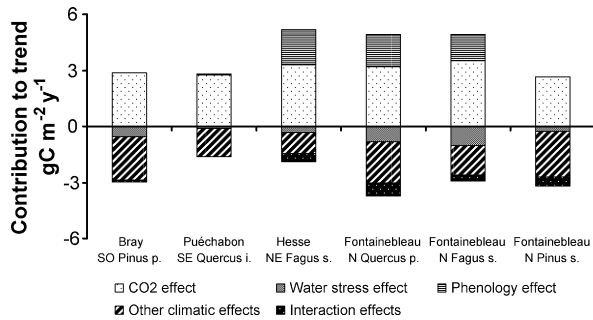
Fig. 8. Summary of the role played by each factor in the determination of the simulated trends defined as the slope of the linear regression of NEP against the year between 1960 and 2100.

"benefits" more of this phenology effect than *F. sylvatica*.

The effect of water stress on NEP (Fig. 7c) varies strongly depending on the site, ranging in average from 20 to 229 g(C) m^{-2} year^{-1}. For all stands, there is a slight decrease of the effect of water stress until 2020–2030 followed by a large increase until 2070 and finally a partial recovery whose intensity depends on the site (Fig. 7c). The slight decrease of the water stress effect until 2020 is mainly caused by the stagnation or slight increase of the summer precipitation combined with a large enhancement of the water use efficiency (Fig. 7b). On the other hand, the decrease of the summer precipitation after 2020 (Fig. 5), leads to an increase of the water stress effect after this date. The amplitude of this increase depends on both the vegetation type (deciduous versus coniferous) as well as the soil extractable water of each stand (Table 2).

The role of water stress in the slowing down of the rate of increase in GPP was also investigated (Fig. 7c and f). While with the drought effect, the increase of GPP after 2020 (all species) corresponds to only 30% of the total GPP rise between 1960 and 2100, this figure rises in average to 60% when the water stress effect is removed. Without the drought effect, GPP increases at a nearly constant rate over the period from 1960 to 2100. With the drought effect, GPP increases much less rapidly after 2020. Based on this analysis, we conclude that the less rapid GPP increase after 2020 is primarily due to the increase in water stress and is not the result of a decrease in the CO$_2$ fertilization effect on carboxylation.

The effect of the changes in atmospheric CO$_2$ concentration is assessed on the carbon and water balances by comparing simulations with and without CO$_2$ increase (Figs. 6 and 7). Without CO$_2$ increase, GPP of deciduous stands increases until 2020 and then decreases or remains stable. In contrast, evergreen forest shows a stable GPP until 2020 followed by a

decrease (less pronounced in *Q. ilex*). Without CO$_2$ increase, R_{eco} increases during the whole period with a smaller slope when compared with simulations including CO$_2$ effects. By comparing runs with and without CO$_2$ effects, we can calculate that CO$_2$ fertilization is responsible from 1960 to 2100 for an NEP enhancement of about 427 g(C) on average for all sites (=3.05 g(C) m^{-2} year^{-1}); i.e., the CO$_2$ fertilization effect turns a decrease of NEP into an increase (Fig. 6c and f). Finally no saturation of this effect on NEP is found because the differences between the simulations with and without CO$_2$ fertilization continuously increase with time (not shown).

In Fig. 8, we summarize the contributions of each factor to the NEP trends. For all ecosystems, the positive effects are mainly due to the CO$_2$ increase. In addition, the lengthening of the leafy period for the deciduous species gives them a considerable "advantage" in comparison to the evergreens. Most of the negative effects are caused by the other climatic effects, especially the temperature effect on ecosystem respiration and perhaps the decrease in relative humidity. For the whole period (1960–2100), the drought effect does not appear as a main factor in explaining the trends. In fact this effect exists but plays a significant role only after 2020 and especially around 2070. It is also interesting to note that the *Q. Ilex* stand is at present already adjusted to water stress and an increase in water shortage does not seem to effect the functioning of this ecosystem. This confirms the weaker effect of increasing water stress and summer time temperature on ecosystems already adapted to a long drought period as reported by Baldocchi (2005). Finally, some effects of the interactions caused by the different factors are highlighted mainly in the northern sites, but the method used does not allow us to determine their nature.

4. Discussion

4.1. Evaluation of the model

CASTANEA has been tested in 1997 in Hesse (Dufrêne et al., 2005; Davi et al., 2005). The present study evaluates its performance over a larger range of climate and tree species. There is a systematic overestimation of NEP for the conifer stands and an underestimation for the *Q. ilex* and *F. sylvatica* stands, but CASTANEA simulates the net ecosystem productivity at least as well (in terms of R^2 and R.M.S.E. see Table 3) as several other models (Kramer et al., 2002) using the same EUROFLUX data set from Bray, Hesse and Loobos. The seasonal pattern of NEP was not

always well captured, especially in the autumn. This is most certainly due to a lack of accuracy in phenology (leaf fall) or to lag effects of drought on photosynthetic parameters in le Bray or respiration in Puéchabon. This confirms the conclusions based on an analysis of data from 1997 in Hesse (Davi et al., 2005) and suggests that further studies concerning the seasonality of the different processes are required (Falge et al., 2002). For the water balance component of the model Davi et al. (2005) have shown that the CASTANEA model gives estimates of ETR superior to eddy-fluxes measurements. However, simulated transpiration is closer to transpiration estimated from sapflow measurements in Hesse. Moreover, by examination of the flux measurements during a drought period (Figs. 1 and 2) or the soil water content (Davi et al., 2005), we conclude that the water stress does not seem to be overestimated.

During the drought period Reichstein et al. (2002) found a strong increase of the modelled WUE at the Puéchabon site, which did not agree with the measurements. Reichstein et al., concluded that it was necessary to revise the way that drought is taken into account in the process-based models. In contrast to the model used in Reichstein et al. (2002) but in agreement with the measurements, CASTANEA simulates a decrease of WUE during drought at the Puéchabon site. But, our model strongly overestimates the night NEP during the water stress period and this overestimation may compensate a hidden overestimation of photosynthesis and may thus be the cause of the good fit of the simulated versus measured NEP. The fact, however that our simulated WUE decreased during the water stress period, questions the results found by Reichstein et al. (2002). As the coupling between photosynthesis and stomatal conductance is similar in both models, the differences of parameterisations between the two studies, both concerning the Ball et al. (1987) coupling and photosynthetic parameters, are probably the cause of these different results (see also Reichstein et al., 2003). Firstly, the Ball et al. (1987) coefficient in well-watered conditions is taken to 15 in Reichstein et al. (2002), while we use the value given by Medlyn et al. (2002) of 6.2. Secondly, Reichstein et al. (2002) use a value near 3.4 for the J_{max}/V_{cmax} ratio (at 20 °C) instead of 2.1 as in our study, a value that is closer to the ones found in the literature (Wullschleger, 1993; Leuning, 1997; Dreyer et al., 2000). During the drought period, the slope of the Ball et al. (1987) relationship decreases, and this could cause WUE to increase. But simultaneously, air relative humidity decreases, leading to an increase in evapora-

tive demand and this can lead to the reduction in simulated WUE (not shown). When changing from a drought period in August to a well watered period at the end of September, the two antagonistic phenomena occur and depending on the amplitude of the decrease of the slope of the Ball et al. relationship, the change of air relative humidity and the photosynthesis sub-model parameterisation, the model predicts either an increase or a decrease of the WUE.

The model has shown to be able to reproduce the various levels of tree growth between the ecosystems and assess their between-year variations. This confirms the result found by Davi (2004), showing that the model is able to reproduce the between-year variations of NEP and TR. On the whole, the prediction accuracy of the model appears sufficient to have confidence in a sensitivity analysis on the impact of climatic change on carbon and water fluxes of forest ecosystems. However, the systematic overestimation of the growth, as well as the biases on daily NEP, must be kept in mind when interpreting the results. Nevertheless, as these biases are systematic, they probably do not change the results concerning the general tendencies observed with change in climate.

4.2. How to explain contrasting responses of CO_2 and H_2O fluxes, between ecosystems?

The response of vegetation to the environment is a key global change issue that scientists are investigating by means of measurements and models on short and long-time scales (Law et al., 2002). There are large differences in life traits between forest ecosystems considered in this study, concerning phenology (date of budburst and life duration), allocation, photosynthetic capacity or amount of respiring tissues. The coniferous species keep their foliar biomass throughout the year. So in temperate climate they do not benefit from an increase in length of the growing season and they ''suffer'' more from the stimulation of the leaf respiration due to temperature increase than the deciduous species (note that this phenomenon is counterbalanced in particular in Boreal regions by the lengthening of the assimilation period). These two causes are more important than water stress in explaining the decrease or stagnation of NEP (Fig. 8). This conclusion remains the same even if we assume that stomatal conductance does not acclimate. This point is highlighted by the simulations of the effect of water stress on NEP without CO_2 increase (Fig. 7f) and consequently without stomatal acclimation.

The ecosystem dominated by *Q. ilex* exhibits a more continuous pattern of NEP dynamics for the entire period of simulation (i.e. 1960–2100). There is a relatively constant increase in GPP, R_{eco} and NEP (except around 2000–2010) and no trends in ETR. In contrast to the other ecosystems, NEP shows a peak during the period 2000–2010, which is mainly due to a GPP increase that is caused by a decrease in the effect of water stress during this period (Fig. 7c). On the other hand, in Puéchabon NEP significantly increases even after 2020. This is mainly caused by the absence of an increase in the effects due to water stress and the smaller negative effects on NEP by the other climate variables than is the case for the coniferous species (Fig. 8).

Unlike the evergreen species, the deciduous species largely benefit of the lengthening of the foliated season and show a strong raise of both NEP and ETR during the first period (until 2020) even when CO_2 fertilization is suppressed (Fig. 6e). During the second period (i.e. 2020–2100), GPP, NEP and ETR decrease or remain stable while the R_{eco} increase continues with the same or a slightly enhanced rate. The differences between the stands arise from an interaction between the level of water stress, temperature and other climatic effects depending both on vegetation (species, age, etc.) and site parameters. In Fontainebleau, the *Q. petraea* stand has a higher leaf biomass (Table 2) than the stand dominated by *F. sylvatica*: this explains its lower NEP (Fig. 6b) despite its higher GPP (Fig. 6a). The difference between the two *F. sylvatica* stands in Hesse and in Fontainebleau is mainly explained by the smaller effect of drought in Hesse (Fig. 8) because of higher SEW and higher precipitation in Hesse.

Even if the role of water stress in the NEP trends between 1960 and 2100 is quantitatively small (Fig. 8), it still explains a part of the variability between sites and the relative slowing down of the photosynthesis after 2020. The temperature increase plays a major role in "favouring" deciduous sites through the increase in the duration of the leafy period, while it has only negative effects for the evergreen species, through the respiration increase. Global radiation and relative humidity changes also explain some differences between sites concerning GPP trends. For all these reasons, even if climatic variables show similar patterns between sites, the evolution of the carbon storage can change according to the species (particularly the distinction between evergreen and deciduous trees), the soil moisture status (determining the SEW) or the stand biomass (acting on respiration level) and soil carbon pools.

Finally the model implicitly assumes a decrease of the stomatal conductance with CO_2 increase. Some

measurements show that the stomatal conductance actually decreases (Curtis, 1996) but this stomatal closure is not always significant and this effect strongly varies in amplitude depending on the species and sites (Medlyn et al., 2002). Consequently the way to simulate the CO_2 effect on the photosynthesis and conductance must be further investigated and validated, particularly to improve the assessment of the effect of water stress (Fig. 7c and f) and the influence upon it by the changes in water use efficiency.

4.3. Perspective and conclusion

In this study an hybrid (SVAT + growth) process-based model is evaluated by comparison with eddy covariance and growth data sets. The effects of climate change derived for 1960–2100 on six forest ecosystems are assessed. This study allows to evaluate the performance of a generic forest model and to highlight the important role of the balance between the ecosystem respiration and the gross photosynthesis in the possible evolution of the carbon storage. The proportion of respiring organs and the phenology type (deciduous or evergreen) mainly explain the differences found between the different ecosystems. On the other hand, the effect of water stress plays a role in the long-term trends by slowing down the GPP rise.

A climatic sensitivity analysis was performed, without considering nitrogen cycle feedback, nitrogen deposition changes, forestry practices or age effects on the modelled net ecosystem productivity, therefore, some conclusions may obviously change, if for instance nitrogen or other nutrients should become the main limiting factor (Kirschbaum et al., 1998). In the very near future, the same approach could be followed using a coupled nitrogen–carbon–water cycle model. More-over, other complementary studies have already also addressed the effects of drought and of forestry practices in the ecosystem functioning (Loustau et al., 2005) and the way to estimate the carbon budget at the regional scale (le Maire et al., 2005).

Even if the generalisation of results is limited by focusing only on six ecosystems, these ecosystems are representative of a significant proportion of forests in western Europe, as three of the main forest types (Mediterranean, temperate deciduous and temperate coniferous) and four main species of western European forest are considered. Cramer et al. (2001) using six global models under the same climatic scenario as is used in our study (but not the same climatic model since they use the outputs from HadCM2-CUL), found a

similar trend in NEP with a large increase until 2030, levelling off after that. However, they conclude that this change of tendency is probably due to saturation of the effect of photosynthesis to high CO_2 levels, while our simulations suggests that photosynthesis stimulation remains high but is not enough to compensate for the large effects of increasing water stress for the deciduous species and respiration increase for the evergreen species. This study demonstrates the usefulness of a process-based model to quantify the relative impact of change in atmospheric CO_2 concentration and of different climatic factors on CO_2 and H_2O exchange between forest ecosystems and the atmosphere. The confidence in our results is strengthened by the validation of the model for the same sites as for which the model was used to simulate the effects of climate change on carbon fluxes and tree growth using climate forecasts for these sites. This gives better insight into the mechanisms that control responses to climate change. The present analysis can be helpful to understand predictions of global scale models, which include simulated vegetation dynamics and are less easily interpretable.

Acknowledgements

Appendix A. Description of sites

A.1. The Hesse site

The experimental plot area is located in the East of France (48°40′N, 7°05′E, altitude 300 m) and is mainly composed of beech (*Fagus sylvatica* L.) with very sparse understorey. The studied plot covers 0.63 ha of a beech forest (30 years old in 1997) with a density of 3482 trees ha^{-1} and a dominant height close to 14 m. The soil type was intermediate between a luvisol and a stagnic luvisol, with a clay content ranged between 25% and 40%. The annual precipitation was 820 mm and

average temperature 9.2 °C. For more details, see Granier et al. (2000a).

A.2. The Bray site

The experimental site is located in the South western of France (44°43′N, 0°46′W, altitude 62 m) and is composed of a homogeneous maritime pine trees (*Pinus pinaster* Ait.) seeded in 1970. The stand density is 520 trees ha^{-1} and the understorey consists mainly of grass (*Molinia coerecula*). The soil is a sandy podzol lying over a hard iron pan. The water table never goes deeper than 200 cm and sometimes during the winter its level could go up to the soil surface (Ogée et al., 2003). This limit to the water drainage can also increase the available water at the beginning of the summer. The climate is temperate oceanic, with an annual mean temperature of 12.5 °C and 930 mm of precipitations and is characterized by a strong seasonal contrast in water conditions. For more details, see Berbigier et al. (2001).

A.3. The Puéchabon site

The experimental site is located in the Puéchabon State Forest in the south of France (43°44′N, 3°35′E, altitude 270 m). This woodland has been managed as a coppice for centuries and the last clear cut was performed in 1942. The vegetation is largely dominated by *Quercus ilex* L. with a sparse understorey mainly composed of a shrubby layer with *Buxus sempervirens* L., *Phyllirea latifolia* L., *Pistacia terebinthus* L. and *Juniperus oxycedrus* L. The stand density is 8500 trees ha^{-1}. The soil is classified as calcareous fersiallitic with a high clay content. The stone and rock fraction is about 90% across the whole-soil profile. The area has a Mediterranean-type climate. Rainfall occurs during autumn and winter with about 75% between September and April. Mean annual precipitation is 883 mm and mean annual temperature is 13.6 °C over the 1984–2002 period. For more details, see Hoff et al. (2002).

A.4. The Loobos site

The forest is an extensive Scots pine forest in the centre of the Netherlands (52°10′N, 5°44′E, altitude 25 m) with an understorey of *Deschampsia flexuosa*. The forest was planted in the beginning of the previous century. The soil is a sandy soil (humus moder) with a 10 cm top layer of organic material. The stand density is 403 trees ha^{-1}. The area has an oceanic-type climate

with a mean annual temperature of 10 °C and mean annual precipitation of 930 mm over the 1995–2004 period.

A.5. The Fontainebleau site

The Fontainebleau forest is located in the south east of Paris in France (48°25′N, 2°40′E, altitude of 120 m). The dominant species are oak (*Quercus petraea* (Matus) Liebl., *Quercus robur* (Matus) Liebl.), beech (*Fagus sylvatica* L.) and Scots pine (*Pinus sylvestris* L.). The climate is temperate with an average annual temperature of 10.2 °C and an average annual precipitation of 720 mm. Most of deciduous stands are located on flat ground (i.e. on windborne sands), while the coniferous stands are found in the hilly part of the forest (i.e. on the sandy Stampian or the sand-stone, with a shallow soil). In this large mixed deciduous forest extended over 17 000 ha, three stands were further studied. The first one is a mature timber stand (7.8 ha and 622 trees ha^{-1}) dominated by *F. sylvatica* on a soil of type luvisol (humus moder). The second stand is dominated by *Q. petraea* (9.2 ha and 1025 trees ha^{-1}) on a soil of type luvisol (humus acid mull). The third one is dominated by *P. sylvestris* (7.8 ha and 530 trees ha^{-1}) on a podzol (humus moder) soil type. For more details, see le Maire et al. (2005).

References

Aubinet, M., Grelle, A., Ibrom, A., Rannik, Ü., Montcrieff, J., Foken, T., Kowalski, A.S., Martin, P.H., Berbigier, P., Bernhofer, Ch., Clement, R., Elbers, J., Granier, A., Grünwald, T., Morgenstern, K., Pilegaard, K., Rebman, C., Snijders, W., Valentini, R., Vesala, T., 2000. Estimates of the annual net carbon and water exchange of European forests: the EUROFLUX methodology. Adv. Ecol. Res. 30, 113–175.

Badeck, F.W., Bondeau, A., Bottcher, K., Doktor, D., Lucht, W., Schaber, J., Sitch, S., 2004. Responses of spring phenology to climate change. New Phytol. 162, 295–309.

Baldocchi, D.D., 2005. The carbon cycle under stress. Nature 437 (22), 483–484.

Baldocchi, D.D., 2003. Assessing the eddy covariance technique for evaluating carbon dioxide exchange rates of ecosystems: past, present and future. Glob. Change Biol. 9, 479–492.

Baldocchi, D.D., Vogel, C.A., 1996. Energy and CO_2 flux densities above and below a temperate broad-leaved forest and a boreal pine forest. Tree Physiol. 16, 5–16.

Barbaroux, C., 2002. Analyse et modélisation des flux de carbone de peuplements forestiers pour la compréhension de la croissance de deux espèces feuillues *Quercus petratea* et *Fagus sylvatica*. Thèse de Doct. en Sci. Univ. Paris-Sud, Orsay, 182 p+annexes.

Becker, M., Nieminen, T.M., Gérémia, F., 1994. Short-term variations and long term changes in oak productivity in northeastern France. The role of climate and atmospheric CO_2. Ann. Forest Sci. 51, 477–492.

Beerling, D.J., 1999. Long-term responses of boreal vegetation to global change: an experimental and modelling investigation. Glob. Change Biol. 5, 55–74.

Beerling, D.J., Kelly, C.K., 1997. Stomatal density responses of temperate woodland plants over the past seven decades of CO_2 increase: a comparison of Salisbury (1927) with contemporary data. Am. J. Bot. 84, 1572–1583.

Berbigier, P., Bonnefond, J.-M., Mellmann, O., 2001. CO_2 and water vapour fluxes for 2 years above Euroflux forest site. Agric. Forest Meteorol. 108, 183–197.

Ball, J.T., Woodrow, I.E., Berry, J.A., 1987. A model predicting stomatal conductance and its contribution to the control of photosynthetis under different environmental conditions. In: Biggins, J. (Ed.), Progress in Photosynthesis Research, vol. 4. pp. 221–224.

Bernacchi, C.J., Singsaas, E.L., Pimentel, C., Portis, A.R., Long, S.P., 2001. Improved temperature response functions for models of Rubisco-limited photosynthesis. Plant Cell Environ. 24, 253–259.

Bosc, A., de Grandcourt, A., Lousteau, D., 2003. Variability of stem and branch maintenance respiration in a *Pinus pinaster* tree. Tree Physiol. 23, 227–236.

Bouriaud, O., 2003. Analyse fonctionnelle de la productivité du hêtre: influences des conditions de milieu, de la structure du peuplement et du couvert, effets de l'éclaircie. Thèse de Doct. en Sciences forestière, ENGREF, 240 p+annexes.

Bradley, R.S., Diaz, H.F., Eischeid, J.K., Jones, P.D., Kelly, P.M., Goodess, C.M., 1987. Precipitation fluctuations over Northern Hemisphere land areas since the mid-19th century. Science 237, 171–175.

Cannell, M.G.R., Thornley, J.H.M., Mobbs, D.C., Friend, A.D., 1998. UK conifer forests may be growing faster in response to increased N deposition, atmospheric CO_2 and temperature. Forestry 71, 277–296.

Ciais, P., Reichstein, M., Viovy, N., Granier, A., Ogee, J., Allard, V., Aubinet, M., Buchmann, N., Bernhofer, C., Carrara, A., Chevallier, F., De Noblet, N., Friend, A.D., Friedlingstein, P., Grunwald, T., Heinesch, B., Keronen, P., Knohl, A., Krinner, G., Loustau, D., Manca, G., Matteucci, G., Miglietta, F., Ourcival, J.M., Papale, D., Pilegaard, K., Rambal, S., Seufert, G., Soussana, J.F., Sanz, M.J., Schulze, E.D., Vesala, T., Valentini, R., 2005. Europe-wide reduction in primary productivity caused by the heat and drought in 2003. Nature 437, 529–533.

Coops, N.C., Waring, R.H., 2001. Assessing forest growth across southwestern Oregon under a range of current and future global change scenarios using a process model, 3-PG. Glob. Change Biol. 7, 15–29.

Courtier, P., Freydier, C., Geleyn, J.F., Rabier, F., Rochas, M., 1991. The ARPEGE project at Météo, France. In: Proceedings of the ECMWF Workshop on Numerical Methods in Atmospheric Modelling, vol. 2. ECMWF, pp. 193–231.

Cramer, W., Kicklighter, D.W., Bondeau, A., Churkina, G., Nemry, B., Ruimy, A., Schloss, A.L., Intercomparison, T.P.O.T.P.N.M., 1999. Comparing global models of terrestrial net primary productivity (NPP): overview and key results. Glob. Change Biol. 5, 1–15.

Cramer, W., Bondeau, A., Woodward, I, Prentice, I.C., Betts, R.A., Brovkin, V., Cox, P.M., Fisher, V., Foley, J., Friend, A.D., Kucharik, C., Lomas, M.R., Ramankutty, N., Sitch, S., Smith, B., White, A., Young-Molling, C., 2001. Global response of terrestrial ecosystem structure and function to CO_2 and climate change: results from six dynamic global vegetation models. Glob. Change Biol. 7, 357–373.

Curtis, P.S., 1996. A meta-analysis of leaf gas exchange and nitrogen in trees grown under elevated carbon dioxide. Plant Cell Environ. 19, 127–137.

Damesin, C., Ceschia, E., Le Goff, N., Ottorini, J.M., Dufrêne, E., 2002. Stem and branch respiration of beech: from tree measurements to estimations at the stand level. New Phytol. 153, 159–172.

D'Arrigo, R.D., Jacoby, G.C., Fung, I.Y., 1987. Boreal forests and atmosphere-biosphere exchange of carbon dioxide. Nature 329, 321–323.

Davi, 2004. Modélisation des flux et des stocks de carbone et d'eau dans les écosystèmes forestiers dans le cadre des changements climatiques: Vers un modèle forestier générique et méthodologie du changement d'échelle (Modelling carbon and water fluxes and stocks in forestry ecosystems in the framework of climate change: towards a generic model). Thèse en écologie fonctionnelle, Université Paris-Sud XI, Paris, France.

Davi, H., Dufrêne, E., Granier, A., Le Dantec, V., Barbaroux, B., François, C., Bréda, N., Montpied, P., 2005. Modelling carbon and water cycles in a beech forest. Part II. Validation for each individual processes from organ to stand scale. Ecol. Model. 185 (2–4), 387–405.

Déqué, M., Marquet, P., Jones, R.G., 1998. Simulation of climate change over Europe using a global variable resolution general circulation model. Clim. Dyn. 14, 173–189.

Déqué, M., Piedelievre, J.P., 1995. High resolution climate simulation over Europe. Clim. Dyn. 11, 321–339.

Déqué, M., Dreveton, C., Braun, A., Cariolle, D., 1994. The ARPEGE/IFS atmosphere model: a contribution to the French community climate modelling. Clim. Dyn. 10, 249–266.

Dolman, A.J., Moors, E.J., Elbers, J.A., 2002. The carbon uptake of a mid latitude pine forest growing on sandy soil. Agric. Forest Meteorol. 111, 157–170.

Dreyer, E., Le Roux, X., Montpied, P., Dautet, F.A., Masson, F., 2000. Temperature response of leaf photosynthetic capacity in seedlings from seven temperate tree species. Tree Physiol. 21, 223–232.

Dufrêne, E., Davi, H., François, C., le Maire, G., Le Dantec, V., Granier, A., 2005. Modelling carbon and water cycles in a Beech forest. Part I. Model description and uncertainty analysis on modelled NEE. Ecol. Modell. 185 (2–4), 407–436.

Ehleringer, J., Björkman, O., 1977. Quantum yields for CO_2 uptake in C3 and C4 plants. Dependence on temperature, CO_2 and O_2 concentration. Plant Physiol. 59, 86–90.

Enjalbal, M., 1994. Etude de l'accroissement radial du chêne vert (*Quercus ilex* L.) relation avec la variabilité climatique dans le bas-Languedoc. DEA, Marseille, 43 pp.

Epron, D., Le Dantec, V., Dufrêne, E., Granier, A., 2001. Seasonal dynamics of soil carbon efflux and simulated rhizosphere respiration in a beech forest. Tree Physiol. 21, 145–152.

Falge, E., Baldocchi, D., Tenhunen, J., Aubinet, M., Bakwin, P., Berbigier, P., Bernhofer, C., Burba, G., Clement, R., Davis, K.J., Elbers, J.A., Goldstein, A.H., Grelle, A., Granier, A., Guomundsson, J., Hollinger, D., Kowalski, A.S., Katul, G., Law, B.E., Malhi, Y., Meyers, T., Monson, R.K., Munger, J.W., Oechel, W., Tha Paw, K., 2002. Seasonality of ecosystem respiration and gross primary production as derived from FLUXNET measurements. Agric. Forest Meteorol. 113, 53–74.

Farquhar, G.D., von Caemmerer, S., Berry, J.A., 1980. A biochemical model of photosynthetic CO_2 assimilation in leaves of C3 species. Planta 149, 78–80.

François, C., 2002. The potential of directional radiometric temperatures for monitoring soil and leaf temperatures and soil moisture status. Remote Sens. Environ. 80 (1), 122–133.

Gibelin, A., Déqué, M., 2003. Anthropogenic climate change over the Mediterranean region simulated by a global variable resolution model. Clim. Dyn. 20, 327–339.

Granier, A., Ceschia, E., Damesin, C., Dufrêne, E., Epron, D., Gross, P., Lebaube, S., Le Dantec, V., Le Goff, N., Lemoine, D., Lucot, E., Ottorini, J.M., Pontailler, J.Y., Saugier, B., 2000a. The carbon balance of a young beech forest. Funct. Ecol. 14, 312–325.

Granier, A., Lousteau, D., Bréda, N., 2000b. A generic model of forest canopy conductance dependent on climate, soil water availability and leaf area index. Ann. Forest Sci. 57, 755–765.

Granier, A., Bréda, N., Biron, P., Villette, S., 1999. A lumped water balance model to evaluate duration and intensity of drought constraints in forest stands. Ecol. Model. 116, 269–283.

Grant, R.F., Nalder, I.A., 2000. Climate change effects on net carbon exchange of a boreal aspen-hazelnut forest: estimates from the ecosystem model *ecosys*. Glob. Change Biol. 6, 183–200.

Guyon, D., Berbigier, P., Courrier, G., Lagouarde, J.P., Moreau, P., 2003. Estimation du LAI dans un écosystème cultivé de pin maritime à partir de mesures de fractions de trouées directionnelles. J. Can. Télédétection 29 (3), 336–348.

Häger, C., Wurth, G., Kohlmaier, G.H., 1999. Biomass of forest stands under climatic change: a German case study with the Frankfurt biosphere model (FBM). Tellus B 51, 385–401.

Hoff, C., Rambal, S., Joffre, R., 2002. Simulating carbon and water flows and growth in a Mediterranean evergreen *Quercus ilex* coppice using the FOREST-BGC model. Forest Ecol. Manage. 164, 121–136.

Idso, S.B., 1981. A set of equations for full spectrum and 8–14 μm and 10.5–12.5 μm thermal radiation from cloudless skies. Water Resource Res. 17 (2), 295–304.

IPCC, 2001. In: Houghton, D., Griggs, N., Van der Linder, D., Maskell, J. (Eds.), Climate Change 2001. The Scientific Basis. Contribution of Working Group I to the Third Assessment Report of the IPCC. Cambridge University Press, Cambridge, UK, p. 881.

Joos, F., Prentice, I.C., House, J.I., 2002. Growth enhancement due to global atmospheric change as predicted by terrestrial ecosystem models: consistent with US forest inventory data. Glob. Change Biol. 8, 299–303.

Kauppi, P.E., Mileikakainen, K., Kuusela, K., 1992. Biomass and carbon budget of European forests, 1971–1990. Science 256 (5053), 70–74.

Kicklighter, D.W., Bruno, M., Donges, S., Esser, G., Heimann, M., Helfrich, J., Ift, F., Joos, F., Kaduk, J., Kohlmaier, G.H., Mcguire, A.D., Melillo, J.M., Meyer, R., Iii, B.M., Nadler, A., Prentice, I.C., Sauf, W., Schloss, A.L., Sitch, S., Wittenberg, U., Wurth, G., 1999. A first-order analysis of the potential role of CO_2 fertilization to affect the global carbon budget: a comparison of four terrestrial biosphere models. Tellus B 51, 343–366.

Kirschbaum, M.U.F., 1999. Modelling forest growth and carbon storage in response to increasing CO_2 and temperature. Tellus B 51, 871–888.

Kirschbaum, M.U.F., Medlyn, B.E., King, D.A., Pongracic, S., Murty, D., Keith, H., Khanna, P.K., Snowdon, P., Raison, R.J., 1998. Modelling forest-growth response to increasing CO_2 concentration in relation to various factors affecting nutrient supply. Glob. Change Biol. 4, 23–41.

Korner, C., 1994. Biomass fractionation in plants: a reconsideration of definitions based on plant functions. In: Roy, J., Garnier, E. (Eds.), A Whole Plant Perspective on Carbon–Nitrogen Interactions. SPB Academic Publishing bv, The Hague, pp. 173–185.

Kramer, K., Leinonen, I., Bartelink, H.H., Berbigier, P., Borghetti, M., Bernhofer, Ch., Cienciala, E., Dolman, A.J., Froer, O., Gracia,

C.A., Granier, A., Grünwald, T., Hari, P., Jans, W., Kellomäki, S., Loustau, D., Magnani, F., Markkanen, T., Matteucci, G., Mohren, G.M.J., Moors, E., Nissinen, A., Peltola, H., Sabaté, S., Sanchez, A., Sontag, M., Valentini, R., Vesala, T., 2002. Evaluation of six process-based forest growth models using eddy-covariance measurements of CO_2 and H_2O fluxes at six forest sites in Europe. Glob. Change Biol. 8 (3), 213–230.

Law, B.E., Falge, E., Gu, L., Baldocchi, D.D., Bakwin, P., Berbigier, P., Davis, K., Dolman, A.J., Falk, M., Fuentes, J.D., Goldstein, A., Granier, A., Grelle, A., Hollinger, D., Janssens, I.A., Jarvis, P., Jensen, N.O., Katul, G., Mahli, Y., Matteucci, G., Meyers, T., Monson, R., Munger, W., Oechel, W., Olson, R., Pilegaard, K., Paw, U.K.T., Thorgeirsson, H., Valentini, R., Verma, S., Vesala, T., Wilson, K., Wofsy, S., 2002. Environmental controls over carbon dioxide and water vapour exchange of terrestrial vegetation. Agric. Forest Meteorol. 113, 97–120.

le Maire, G., Davi, H., Soudani, K., François, C., Le Dantec, V., Dufrêne, E., 2005. Modelling annual production and carbon dioxide fluxes of a large managed temperate forest using forest inventories, satellite data and field measurements. Tree Physiol. 25, 859–872.

Leuning, R., 1997. Scaling to common temperature improves the correlation between the photosynthesis parameters Jmax and Vcmax. J. Exp. Bot. 48, 345–347.

Leuning, R., Moncrieff, J., 1990. Eddy-covariance CO_2 flux measurements using open-path and close path CO_2 analysers. Corrections for analyser water vapour sensitivity and damping of fluctuations in air sampling tubes. Bound. Layer Meteorol. 53, 63–67.

Liozon, R., Badeck, F.W., Genty, B., Meyer, S., Saugier, B., 2000. Leaf photosynthetic characteristics of beech (*Fagus sylvatica* L.) saplings during three years of exposure to elevated CO_2 concentration. Tree Physiol. 20, 239–247.

Long, S.P., 1991. Modification of the response of photosynthetic productivity to rising temperature by atmospheric CO_2 concentration: has its importance been underestimated? Plant Cell Environ. 14, 729–739.

Loustau, D., Bosc, A., Colin, A., Davi, H., François, C., Dufrêne, E., Déqué, M., Cloppet, E., Arrouays, D., le Bas, C., 2005. Modelling the climate change effects on the potential production of French plains forests at the sub regional level. Tree Physiol. 25, 813–823.

Medlyn, B.E., Lousteau, D., Delzon, S., 2002. Temperature response of parameters of a biochemically based model of photosynthesis. I. Seasonal changes in mature maritime pine (*Pinus pinaster* Ait.). Plant Cell Environ. 25, 1155–1165.

Medlyn, B.E., Barton, C.V.M., Broadmeadow, M.S.J., Ceulemans, R., De Angelis, P., Forstreuter, M., Freeman, M., Jackson, S.B., Kellomäki, S., Laitat, E., Rey, A., Roberntz, P., Sigurdsson, B.D., Strassemeyer, J., Wang, K., Curtis, P.S., Jarvis, P.G., 2001. Stomatal conductance of forest species after long-term exposure to elevated CO_2 concentration: a synthesis. New Phytol. 149, 247–264.

Medlyn, B.E., Jarvis, P.G., 1999. Design and use of a database of model parameters from elevated [CO_2] experiments. Ecol. Model. 124, 69–83.

Meiresonne, L., Sampson, D.A., Kowalski, A.S., Janssens, I.A., Nadezhdina, N., Cermak, J., Van Slycken, J., Ceulemans, R., 2003. Water flux estimates from a Belgian Scots pine stand: a comparison of different approaches. J. Hydrol. 270, 230–252.

Minkkinen, K., Korhonen, R., Savolainen, I., Laine, J., 2002. Carbon balance and radiative forcing of Finnish peatlands 1900–2100—the impact of forestry drainage. Glob. Change Biol. 8, 785–799.

Montcrieff, J.B., Mahli, Y., Leuning, R., 1996. The propagation of errors in long term measurements of land-atmosphere fluxes of carbon and water. Glob. Change Biol. 2, 231–240.

Monteith, J.L., 1965. Evaporation and environment. In: The State and Movement of Water in Living Organisms, XIX TII Symposium of the Society for Experimental Biology. Cambridge University Press, New York, pp. 205–233.

Myneni, R.B., Dong, J., Tucker, C.J., Kaufmann, R.K., Kauppi, P.E., Liski, J., Zhou, L., Alexeyev, V., Hughes, M.K., 2001. A large carbon sink in the woody biomass of northern forests. Proc. Natl. Acad. Sci. U.S.A. 98 (26), 14784–14789.

Nabuurs, G.J., Schelhaas, M.J., Mohren, G.F.M.J., Field, C.B., 2003. Temporal evolution of the European forest sector carbon sink from 1950 to 1999. Glob. Change Biol. 9, 152–160.

Nabuurs, G.J., Pussinen, A., Karjalainen, T., Erhard, M., Kramer, K., 2002. Stemwood volume increment changes in European forests due to climate change—a simulation study with the EFISCEN model. Glob. Change Biol. 8, 304–316.

Nolan, W.G., Smillie, R.M., 1976. Multi-temperature effects on Hill reaction, activity of barley chloroplasts. Biochim. Biophys. Acta 440, 461–475.

Ogée, J., Brunet, Y., Lousteau, D., Berbigier, P., Delzon, S., 2003. MuSICA, a CO_2, water and energy multilayer, multileaf pine forest model: evaluation from hourly to yearly time scales and sensitivity analysis. Glob. Change Biol. 9, 697–717.

Parton, W.J., Schimel, D.S., Cole, C.V., Ojima, D.S., 1987. Analysis of factors controlling soil organic matters levels in great plains grasslands. Soil Sci. Soc. Am. J. 51, 1173–1179.

Penning de Vries, F.W.T., 1975a. Use of assimilates in higher plants. In: Cooper, J.P. (Ed.), Photosynthesis and Productivity in Different Environments: International Biological Programme 3. Cambridge University Press, Londres, pp. 459–480.

Penning de Vries, F.W.T., 1975b. The cost of maintenance processes in plant cells. Ann. Bot. 39, 77–92.

Penning de Vries, F.W.T., Brunsting, A.H.M., Van Laar, H.H., 1974. Products, requirement and efficiency of biosynthesis: a quantitative approach. J. Theor. Biol. 45, 339–377.

Porté, A., 1999. Modélisation des effets du bilan hydrique sur la production primaire et la croissance d'un couvert de pins maritime (*Pinus pnaster* Aït.) en lande humide. Ph.D. Thesis. Université d'Orsay-Paris XI, Orsay.

Rambal, S., Ourcival, J.-M., Joffre, R., Mouillot, F., Nouvellon, Y., Reichstein, M., Rocheteau, A., 2003. Drought controls over conductance and assimilation of a Mediterranean evergreen ecosystem: scaling from leaf to canopy. Glob. Change Biol. 9 (12), 1813–1824.

Rapp, M., Lossaint, P., 1978. La forêt méditerranéenne de chêne verts (*Quercus ilex* L.).In: Problèmes d'Ecologie: écosystèmes terrestres, Paris, pp. 129–185.

Reichstein, M., Tenhunen, J.D., Roupsard, O., Ourcival, J.M., Rambal, S., Miglietta, F., Peressotti, A., Pecchiaris, M., Tirone, G., Valentini, R., 2002. Severe drought effect on ecosystem CO_2 and H_2O fluxes at three Mediterranean evergreen sites: revision of current hypotheses? Glob. Change Biol. 8, 999–1017.

Reichstein, M., Tenhunen, J., Ourcival, J.M., Rambal, S., Roupsard, O., Miglietta, F., Pecchiari, M., Peressotti, A., Tirone, G., Valentini, R., 2003. Inverse modelling of seasonal drought effects on canopy CO_2/H_2O exchange in three Mediterranean ecosystems. J. Geophys. Res. 108 (D3), 4726.

Ryan, G.M., 1991. Effects of climate change on plant respiration. Ecol. Appl. 1 (2), 157–167.

Sala, A., Tenhunen, J.D., 1996. Simulations of canopy net photosynthesis and transpiration in *Quercus ilex* L. under the influence of seasonal drought. Agric. Forest Meteorol. 78, 203–222.

Sellers, P.J., Dickinson, R.E., Randall, D.A., Betts, A.K., Hall, F.G., Berry, J.A., Collatz, G.J., Denning, A.S., Mooney, H.A., Nobre, C.A., Sato, N., Field, C.B., Henderson-Sellers, A., 1997. Modeling the exchanges of energy, water, and carbon between continents and the atmosphere. Science 275, 502–509.

Spitters, C.J.T., 1986. Separating the diffuse and direct component of global radiation and its implications for modelling canopy photosynthesis. Part II. Calculation of canopy photosynthesis. Agric. Forest Meteorol. 38, 231–242.

Spitters, C.J.T., Toussaint, H.A.J.M., Goudriaan, J., 1986. Separating the diffuse and direct component of global radiation and its implications for modelling canopy photosynthesis. Part I. Components of incoming radiation. Agric. Forest Meteorol. 38, 217–229.

Sternberg, P., 1996. Correcting LAI-2000 estimates for the clumpong of needle in shoots of conifers. Agric. Forest Meteorol. 79, 1–8.

Valentini, R., 1999. The role of flux monitoring networks in carbon dioxide source/sinks estimation in terrestrial ecosystems. In: Valentini, R., Brüning, C. (Eds.), Greenhouse Gases and their Role in Climate Change: The Status of Research in Europe. European Commission DG XII/B I EUR (19085 EN), pp. 1–6.

Verhoef, W., 1984. Light scattering by leaf layers with application to canopy reflectance modeling: the SAIL model. Remote Sens. Environ. 16, 125–141.

Verhoef, W., 1985. Earth observation modelling based on layer scattering matrices. Remote Sens. Environ. 17, 165–178.

White, A., Cannell, M.G.R., Friend, A.D., 2000a. CO_2 stabilization, climate change and the terrestrial carbon sink. Glob. Change Biol. 6, 817–833.

White, A., Cannell, M.G.R., Friend, A.D., 2000b. The high-latitude terrestrial carbon sink: a model analysis. Glob. Change Biol. 6, 227–245.

Wullschleger, S.D., 1993. Biochemical limitations to carbon assimilation in C3 plants—a retrospective analysis of the A/Ci curves from 109 species. J. Exp. Bot. 44, 907–920.